

Helicity dynamics, inverse and bi-directional cascades in fluid and MHD turbulence: A brief review

A. Pouquet^{1,2}, D. Rosenberg³, J.E. Stawarz⁴ and R. Marino⁵

¹Laboratory for Atmospheric and Space Physics, Boulder, CO 80309 USA.

²NCAR, P.O. Box 3000, Boulder, CO 80307 USA.

³NOAA, Boulder, CO, United States.

⁴Department of Physics, Imperial College London, United Kingdom.

⁵Laboratoire de Mécanique des Fluides et d'Acoustique, CNRS, École Centrale de Lyon, Université de Lyon, INSA de Lyon, Écully, 69134, France

Key Points:

- Magnetic helicity displays an inverse cascade to large scales which, in electron MHD, can be justified with a simple phenomenological model
- Total energy in MHD or rotating stratified turbulence has constant-flux cascades to small and large scale, affecting mixing and dissipation
- With these results, needed modifications to sub-grid scale turbulence models will be enhanced using tools from big-data and machine-learning

Abstract

We briefly review helicity dynamics, inverse and bi-directional cascades in fluid and magnetohydrodynamic (MHD) turbulence, with an emphasis on the latter. The energy of a turbulent system, an invariant in the non-dissipative case, is transferred to small scales through nonlinear mode coupling. Fifty years ago, it was realized that, for a two-dimensional fluid, energy cascades instead to larger scales, and so does magnetic helicity in three-dimensional MHD. However, evidence obtained recently indicates that in fact, for a range of governing parameters, there are systems for which their ideal invariants can be transferred, with constant fluxes, to both the large scales and the small scales, as for MHD or rotating stratified flows, in the latter case including with quasi-geostrophic forcing. Such bi-directional, split, cascades directly affect the rate at which mixing and dissipation occur in these flows in which nonlinear eddies interact with fast waves with anisotropic dispersion laws, due for example to imposed rotation, stratification or uniform magnetic fields. The directions of cascades can be obtained in some cases through the use of phenomenological arguments, one of which we derive here following classical lines in the case of the inverse magnetic helicity cascade in electron MHD. With more highly-resolved data sets stemming from large laboratory experiments, high-performance computing and in-situ satellite observations, machine-learning tools are bringing novel perspectives to turbulence research, *e.g.* in helping devise new explicit sub-grid scale parameterizations, which may lead to enhanced physical insight, including in the future in the case of these new bi-directional cascades.

Plain-language Summary Turbulent flows are prevalent in Geophysics and Space Physics. They are complex and involve interactions between fluctuations at widely separated scales, with the energy expected in the general case to flow only to small scales where it is dissipated. It was found recently that, contrary to such expectations, energy can go in substantial amounts to both the small and to the large scales, in the presence of magnetic fields, as applicable to space plasmas, and for rotating stratified flows as encountered in the atmosphere and the oceans. This result implies that the amount of energy available for dissipation may differ from flow to flow and simple scaling arguments allow for predictions that are backed up by results stemming from direct numerical simulations. One should incorporate this bi-directional cascade phenomenon in the turbulence models used for global computations of geophysical and astrophysical media. Furthermore, machine-learning tools may prove useful in deriving such enhanced models in their capacity to interrogate the large data bases that already exist for such complex flows.

1 Introduction

Turbulence prevails in many geophysical and astrophysical flows, and progress is being made presently in the understanding of such flows for fluids, neutral or conducting, including in the presence of waves stemming from strong rotation, stratification, compressibility or quasi-uniform magnetic fields. The complexity of turbulent flows comes from the nonlinearity of the underlying equations leading to multi-scale interactions through mode coupling. It can result in a non-universality of spectra in models of MHD, with applications to Solar Wind turbulence [Galtier, 2012] or laboratory plasmas [Bratanov *et al.*, 2013]. It is also at the source of a wide variety of behavior, from the appearance at small scales of sharp structures such as tornadoes, to large-scale pattern formation and coherent vortices. This type of ordered motions at large scale is not limited to physical systems. For example, it is also encountered in micro-biology where it involves the collective behavior within so-called active fluids (see Reinken *et al.* [2018] and references therein, in a fast-moving domain of research), involving interactions between the solvent (say, water) and self-propelled micro-organisms such as amoebae [Wensink *et al.*, 2012].

Substantial advances in the understanding of nonlinear systems have dealt with the zero-dimensional case in which temporal chaos in an otherwise spatially ordered field is observed in many instances, together with fractal behavior, leading to remarkable scaling laws (see several reviews in this Special Issue). Similarly, in one spatial dimension, solitons can arise through an exact balance between nonlinear steepening, due for example to advection, and dispersion, as in the Korteweg-de-Vries or Kuramoto-Sivashinsky equations. Finally, in higher spatial dimensions, the seminal discovery, first for two-dimensional neutral fluids [Kraichnan, 1967] of the possibility of an inverse cascade, that is of excitation reaching scales larger than the forcing scale because of constraints due to the presence of more than one ideal quadratic invariant in the non-dissipative case, has led to a fundamentally different view of turbulent flows beyond the venue that mode-coupling offers for energy dissipation in the small scales.

Inverse and direct cascades are found in other systems, such as nonlinear optics. For example in *Newell and Zakharov* [2008], a direct connection to dissipation at small scales through instabilities of coherent structures at large scales is stressed in such a context. Indeed, in the presence of an inverse cascade leading to instabilities of these large-scale coherent structures, one prediction of weak turbulence – that is, turbulence with waves that are faster than nonlinear eddies – is that there is stronger intermittency in the small scales. This enhanced intermittency can take the form of wave breaking which is often observed for example at the surface of the ocean. Moreover, in weak MHD turbulence in the presence of a strong uniform magnetic field, small-scale intermittency is found as well, together with nonlocal coupling of scales [Meyrand *et al.*, 2015]. In weak Langmuir turbulence, such a coupling between large-scale coherent structures, formed by an inverse cascade in the form of Langmuir cavitons, and strong small-scale turbulence, is also advocated in the coupling of these two forms of turbulence [Henri *et al.*, 2011]. Similarly, the non-Gaussian wings observed for example in four-wave interactions for Langmuir waves are associated with wave breaking, and intermittency is stronger when the linear and nonlinear characteristic times become comparable [Choi *et al.*, 2005]. A simple model of such a strong intermittency, that appears in the vertical velocity of rotating stratified flows, can be developed for a Philipps saturation spectrum [Rorai *et al.*, 2014; Feraco *et al.*, 2018], or when the shorter time-scale of the problem is that associated with random sweeping [Clark *di Leoni* *et al.*, 2017].

These new results are due to a combination of technological, observational, numerical and theoretical advances, for example with the help of several large-scale laboratory experiments such as the Coriolis table to study rapidly rotating turbulence, in the presence or absence of stratification [Aubourg *et al.*, 2017]. Similarly, high values of the control parameter, namely the Reynolds number which measures the relative strength of nonlinearities to (linear) dissipation, are achieved nowadays using liquid helium [*Collaboration SHREK: B. Saint-Michel et al.*, 2014]. At the same time, a multitude of observations are increasing our understanding of such complex fluids, with various space missions [Marino *et al.*, 2008, 2011; Tsurutani *et al.*, 2016], now including using data stemming from MMS (Magnetospheric Multi-Scale, see *e.g.* Wilder *et al.* [2016]), looking at turbulence in the magnetotail [Ergun *et al.*, 2018] or in the magnetosheath [Gershman *et al.*, 2018], as well as in the Solar Wind in general [Chasapis *et al.*, 2017].

Such studies can lead to advance warnings of strong solar eruptions and their ensuing disruption on satellite communications [Cassak *et al.*, 2017]. In parallel, progress in high-performance computing is allowing for numerical simulations at Reynolds numbers that were not explored before with sufficient accuracy in the absence of modeling terms [*de Bruyn Kops*, 2015; Rosenberg *et al.*, 2015; Ishihara *et al.*, 2016; Iyer *et al.*, 2017]. And a renewal of interest in the theory of weak turbulence has allowed for the exploration of small-scale and large-scale intermittency as diagnosed in the oc-

cence of extreme events, such as fronts and filaments in the ocean [McWilliams, 2016], or current sheets in MHD [Zhou *et al.*, 2004; Mininni *et al.*, 2006], as well as shocks in compressible flows [Porter *et al.*, 2002], all events making such flows largely unpredictable. A picture of turbulence is thus emerging that broadens our understanding which, in some instances, dates back to the mid forties for fully developed turbulence (FDT), for example concerning the possible scaling laws for energy spectra, classically compared to the Kolmogorov law for the (kinetic) energy spectrum, namely $E_V(k) \sim \epsilon_V^{2/3} k^{-5/3}$, where k is the isotropic wavenumber and ϵ_V the kinetic energy dissipation rate. It is in this context that we now review results on helicity, and on inverse and bi-directional cascades in MHD and fluid turbulence, with an emphasis on the former.

2 The role of kinetic helicity

We first recall here the general properties of kinetic helicity, H_V , in fluid turbulence. It is defined as the space-integrated correlation between the velocity field \mathbf{u} and the vorticity $\omega = \nabla \times \mathbf{u}$, and is an invariant of the ideal equations of motion for FDT, as well as for purely rotating flows. Note that helicity is not definite positive: it can be of either sign, representing a (partial) alignment or anti-alignment of velocity and vorticity. Helicity has been studied extensively in the laboratory and in numerical simulations [Moffatt and Tsinober, 1992; Biferale *et al.*, 2012], including in the presence of rotation or stratification. Helicity has recently been observed in the laboratory thanks to helicoid particles [Gustavsson and Biferale, 2016], that is particles which are sensitive to the lack of mirror symmetry of the flow in which they are embedded. Hurricanes are associated with strong helicity, since they can be viewed as a quasi two-dimensional rotating stratified flow, thus with mostly vertical vorticity, together with a strong updraft or downdraft [Molinari and Vollaro, 2010]. Helicity is produced by geostrophic balance between the Coriolis force, gravity and pressure gradients [Hide, 2002; Marino *et al.*, 2013], while neglecting the nonlinear advection terms. In tropical storms, helicity is associated with the presence of coherent structures in the form of roll vortices in the boundary layer of typhoons, structures which are linked with inflection-point shear instabilities [Morrison *et al.*, 2005]. Similarly, at river confluences, large-scale turbulence structures are produced in the form of stream-wise oriented helical vortical eddies. When such structures are observed, the mixing properties downstream of the confluence and the mixing interface between the two volumes of water, sometimes of quite different turbidity and salinity, are altered; helical structures also interact with shear layers, leading to the formation of turbulent motions [Constantinescu *et al.*, 2011]. Moreover, helicity can lead to large-scale instabilities [Frisch *et al.*, 1987; Levina and Montgomery, 2014; Yokoi and Brandenburg, 2016], and it has been shown to slow-down the temporal evolution of shear flows, necessitating a change in the modeling formalism of the unresolved small scales, by including turbulent transport coefficients that are helicity-dependent [Yokoi and Yoshizawa, 1993; Baerenzung *et al.*, 2008].

Defining spectral densities of energy and helicity in terms of isotropic wavenumber k , $[E_V(k), H_V(k)]$, and with $\langle \mathbf{u} \cdot \mathbf{u} \rangle / 2 = \int E_V(k) dk$, $\langle \mathbf{u} \cdot \omega \rangle / 2 = \int H_V(k) dk$ the total kinetic energy and helicity, one has a constraint, namely $-1 \leq \sigma_V(k) = H_V(k) / [k E_V(k)] \leq 1$ for the so-called relative helicity density $\sigma_V(k)$, using a Cauchy-Schwarz inequality. In FDT, both $E_V(k)$ and $H_V(k)$ follow a $k^{-5/3}$ spectral law and thus the return to isotropy in homogeneous isotropic turbulence, with full recovery of mirror symmetry ($\sigma_V(k) \rightarrow 0$), occurs at a rate proportional to $1/k$ as $k \rightarrow \infty$.

The analysis of triad interactions decomposed into two circularly polarized (\pm) helical modes as done in Waleffe [1992] shows that an inverse transfer of energy to larger scales takes place when the two small-scale modes of a given triad have the same helical polarity. Although overall the energy cascade is to the small scales, as predicted

in *Kraichnan* [1973], this feature was exploited in *Biferale et al.* [2012] by restricting interactions to one-signed helical modes and observing numerically an inverse cascade of energy in that truncated case. This result further led to the derivation of global regularity in such truncated systems [*Biferale and Titi*, 2013]. A further and rather intriguing result, as analyzed in *Alexakis* [2017], is that in fact, the total energy flux can be decomposed into three different fluxes that are individually constant in the inertial range, hinting at some, as yet undetermined, invariants and, as pointed out in the paper, leading to additional exact laws in terms of third-order structure functions. Similarly, the helicity flux can be partitioned in two independently constant partial fluxes, indicative that the behavior of such flows is more constrained than thought previously. Does this correspond to the separate invariance of the \pm energies of these modes, similarly to the case of MHD where the invariance of total energy and cross helicity, namely $E_T = E_V + E_M$ and $H_C = \langle \mathbf{u} \cdot \mathbf{b} \rangle$, can be expressed as two definite-positive invariants, in the ideal, non-dissipative case, in terms now of the so-called Elsässer variables $\mathbf{z}_\pm = \mathbf{u} \pm \mathbf{b}$, of energies E_\pm . So the question arises as to whether there are also in MHD sub-fluxes that are independently constant in the inertial range, a point open for future research.

Recently, it was also shown in *Stomka and Dunkel* [2017] that, in the context of bacterial suspensions and using the Navier-Stokes equations for the solvent with a stress tensor including higher-order terms modeling the role of the non-Newtonian active part of the fluid, an accumulation of energy at large scales occurred because of an instability due to the bi-Laplacian forcing. One peculiar feature of these solutions is that they can be fully helical, Beltrami flows, $\omega = \lambda \mathbf{v}$ by selecting the scales for which the three linear terms (proportional in Fourier space to k^{2n} , $n = 1, 2, 3$) can balance each other exactly. Note that this corresponds to a viscous-forcing-dissipation balance, somewhat similar to the large-scale quasi-geostrophic equilibrium in rotating stratified flows involving, rather, dispersive effect of inertia-gravity waves and the pressure gradient. Such an inverse energy cascade occurs through spontaneous mirror-symmetry breaking as being the cause of the selection of triadic interactions. Indeed, these new terms in the stress tensor can induce, when the equation is linearized, instabilities of the large scales because of a limited range of unstable Fourier modes depending on the governing parameters.

3 Coupling to a magnetic field

3.1 The direct cascade of energy to small scales

In three-dimensional MHD, the ideal invariants in the absence of dissipation are the total energy $E_T = E_V + E_M = 1/2 \langle |\mathbf{u}|^2 + |\mathbf{b}|^2 \rangle$, the magnetic helicity $H_M = \langle \mathbf{a} \cdot \mathbf{b} \rangle$ with $\mathbf{b} = \nabla \times \mathbf{a}$ (where \mathbf{a} is the magnetic vector potential), and the cross-correlation between the velocity and magnetic field, $H_C = \langle \mathbf{u} \cdot \mathbf{b} \rangle$ [*Woltjer*, 1960; *Pouquet*, 1996; *Blackman*, 2015]. The total energy cascades to small scales, both in two and in three dimensions, with a self-similar spectrum whose spectral index might still be in dispute [*Mininni and Pouquet*, 2007; *Lee et al.*, 2010; *Beresniak*, 2014; *Perez et al.*, 2014], a matter that is rendered difficult (i) by the anisotropy of such flows especially in the small scales because of the presence of a uniform (or quasi-uniform) strong magnetic field in the large scales; (ii) by the presence of correlations between the velocity and the magnetic field, as well as (iii) by intermittency steepening these spectra. Indeed, the intermittency in MHD is known to be stronger than for FDT fluids, and to be variable as well; for example, the anomalous exponents for the scaling of structure functions depend on the intensity of solar flares [*Abramenko and Yurchyshyn*, 2010]. Energy spectra have been observed in the Solar Wind consistently over the years (see *e.g.* *Matthaeus and Goldstein* [1982]; *Marino et al.* [2008]; *Veltri et al.* [2009]). They correspond to a direct energy cascade which leads to plasma heating [*Stawarz et al.*, 2009; *Marino et al.*, 2011] through reconnection events of current and vorticity sheets,

as detected for example in the Solar Wind and the magnetosphere [Phan *et al.*, 2018]. However, there are a variety of possible mechanisms for the dissipation of turbulence in collisionless space plasmas, such as current driven instabilities [Stawarz *et al.*, 2015], and it is still an open question as to what are the dominant mechanisms. Reconnection is also present in numerous numerical studies (see *e.g.* Ting *et al.* [1986]; Zhou *et al.* [2004]; Mininni *et al.* [2006]; Higashimori *et al.* [2013]; Karimabadi *et al.* [2013]; Loureiro *et al.* [2013]), and in plasma relaxation processes [Taylor, 1986].

The observation of magnetic fields in planets and stars, in the interstellar medium or in galaxies leads to the question of their origin. They may be primordial remnants from the early universe, or they may arise from a generation mechanism from a seed field \mathbf{b} coupled to the velocity, through what is called the dynamo effect. Reversals of the geomagnetic field occur in a rather reproducible way, on average, with fast growth and slower decay phases that are comparable between different geological periods [Valet and Fournier, 2016]. It has been known, since Parker's model and the mean field theory developed in Steenbeck *et al.* [1966], that helicity is an essential ingredient of such a dynamo mechanism for creating large-scale fields. Note however that one can find examples of non-helical dynamos which can take place through chaotic stretching of magnetic field lines (see *e.g.* Childress and Gilbert [1995]; Nore *et al.* [1997]). Once a strong magnetic field is generated, it leads to wave propagation and to a weak turbulence regime which has been detected in the magnetosphere of Jupiter [Saur *et al.*, 2002]. It also leads to the development of localized vorticity and current sheets which further roll-up as the turbulence increases for sufficiently high Reynolds numbers [Lee *et al.*, 2010], as observed for example in the Earth's magnetosphere [Alexandrova *et al.*, 2006; Osman *et al.*, 2014].

The decay of energy is lessened in the presence of cross-helicity, *i.e.* the correlations between the velocity and the magnetic field [Pouquet *et al.*, 1988]; this corresponds again to an alignment, here of the velocity and the magnetic field, which weakens the nonlinear terms, directly for Ohm's law, and indirectly for the Lamb vector $\mathbf{u} \times \omega$ which can be compensated exactly, when the correlations are strong, by the Lorentz force $\mathbf{b} \times \mathbf{j}$. Note that the role of anisotropy is central in the dynamics of the cross-correlation, as shown in Briard and Gomez [2018] using a two-point closure of MHD turbulence; it should be investigated further.

3.2 Inverse cascade of magnetic helicity

Magnetic helicity is observed in the solar photosphere (see *e.g.* Blackman [2015] and references therein), and in the Solar Wind [Howes and Quataert, 2010]. Its dynamical role in coronal mass ejections can be modeled through the twisting and reconnection of magnetic flux tubes [Gibson and Fan, 2008; Malapaka and Müller, 2013], and it is known to undergo an inverse cascade to large scales [Frisch *et al.*, 1975; Pouquet *et al.*, 1976; Pouquet, 1993, 1996].

In Figure 1, we give first an illustration of the temporal development of the magnetic energy and helicity spectra, $H_M(k)$, $E_M(k)$ in MHD (top left and right), and the kinetic energy spectra, $E_V(k)$, bottom left. Forcing is for $k_F \approx 20$, and times are indicated in the insert, in units of the turnover time $\tau_{NL} = L_0/U_0$, with U_0, L_0 characteristic velocities and length scales. Dash lines are indicative of possible scaling. One observes the progressive build-up of H_M at large scale which entrains the magnetic energy, since $E_M(k) \geq k|H_M(k)|$; this build-up of magnetic energy then leads to a similar growth of kinetic energy at large scales because of the effect of Alfvén waves [Pouquet *et al.*, 1976]. The Geophysical High-Order Suite for Turbulence (GHOST) code was used (see Stawarz and Pouquet [2015] for details). We also show small-scale current structures drawn at peak of dissipation in the presence of a Hall current (bottom right of Fig. 1). Here, the run is unforced, with random initial conditions, and

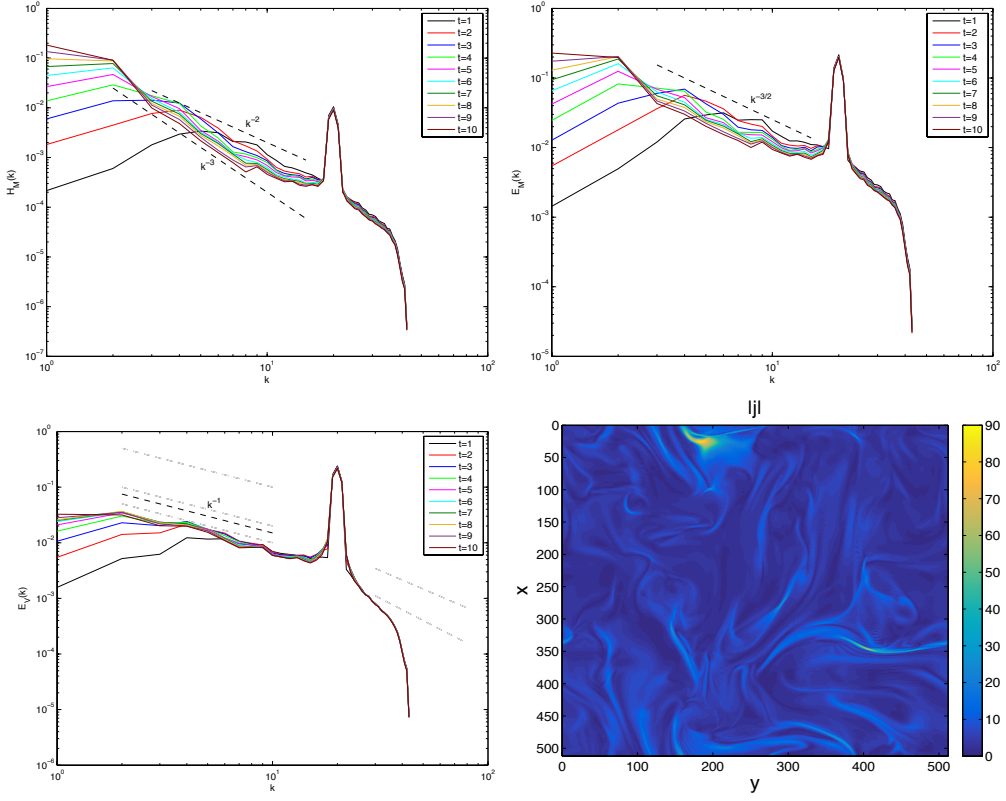


Figure 1. MHD. Spectra in forced MHD turbulence at different times for magnetic helicity and energy (top left and right), and for kinetic energy (bottom left). Bottom right: horizontal cut of the current density in Hall-MHD (see *Stawarz and Pouquet* [2015]).

it is performed on a grid of 512^3 points. Note the strong localized structures. The Hall MHD equations differ from electron MHD, which is discussed below, with the latter being a simplification of the former where one assumes that protons are stationary, an hypothesis which is potentially valid for the small scales of Hall MHD.

3.3 Phenomenology of the inverse cascade for electron MHD

One can argue that, since small scales have shorter timescales, the invariant with the smallest number of derivatives, here the magnetic helicity, goes to the large scales and the other invariant, here the total energy, to the small scales. Such large-scale helical structures in MHD are observed, including in the case when the forcing is non-helical, and their life-time is directly linked to the temporal correlation time of the forcing function [*Dallas and Alexakis*, 2015]. Because such large-scale energetic structures are force-free, it poses the question of a possible linearization of turbulent flows around such stable states in plasma relaxation processes [*Taylor*, 1986]. Magnetic helicity is also detected in the laboratory in perhaps the simplest instance of the family of models for plasmas, namely electron MHD (EMHD) [*Stenzel et al.*, 1995]. In that case, the velocity of the electrons is slaved to the electric current (while ignoring protons), and the resulting equations only involve the magnetic induction \mathbf{B} ; the equations are, with $\mathbf{J} = \nabla \times \mathbf{B}$ the current density:

$$\frac{\partial \mathbf{B}}{\partial t} + \alpha \nabla \times [\mathbf{J} \times \mathbf{B}] = \lambda \nabla^2 \mathbf{B} , \quad \alpha = \frac{c}{4\pi n_e e} , \quad (1)$$

with c the speed of light, n_e the electron density of charge e , and λ the magnetic diffusivity. In the absence of dissipation, the magnetic energy E_M and the magnetic helicity H_M are conserved, and one has $|\sigma_M(k)| \leq 1$, with $\sigma_M(k) = kH_M(k)/E_M(k)$; $\sigma_M = \pm 1$ corresponds to the alignment (or anti-alignment) of the vector potential and the magnetic induction.

As in MHD, waves can travel along an imposed strong magnetic field, in either direction; the so-called *unbalanced* case is when more waves travel in one direction than in the other one. Since the waves in EMHD are circularly polarized, the unbalanced case results in a non-zero magnetic helicity, and thus in an inverse cascade of H_M and direct cascade of E_M . Using DNS of decaying EMHD in 3D, it is shown in *Cho* [2011] that the peak of the magnetic energy spectrum moves to larger scales; this is consistent with the fact that $|\sigma_M(k)| \leq 1$, and the magnetic helicity undergoes an inverse cascade in the forced case. The sign of the energy flux was indeed predicted to be positive in the framework of weak turbulence for EMHD [*Galtier and Bhattacharjee*, 2003].

An argument for the inverse cascade can be made following what is done in *Fjørtoft* [1953] for two-dimensional neutral fluids, since magnetic energy and helicity are dimensionally linked, with $|\sigma_M(k)| \leq 1$. However, to be able to straightforwardly extend the result of Fjørtoft in that case, one needs to assume that helicity is of a given sign and that it is maximal (see *e.g.* *Waleffe* [1992]; *Chen et al.* [2003]; *Slomka and Dunkel* [2017] for detailed analyses of triadic interactions in helical flows). This applies to the set-up of the inverse energy cascade found for one-sign helical flows [*Biferale et al.*, 2012]. Moreover, within the large-scale helical range, the helicity is likely to be of one sign only and in MHD at least it is known to be maximal in the largest scales, corresponding to force-free field configurations [*Pouquet et al.*, 1976]. For the EMHD system, let us assume that we have an exchange of magnetic energy and of magnetic helicity for the triplet of wavenumbers $[k, p = 2k, q = 4k]$, written as $\delta E_{M,kpq}$ and $\delta H_{M,kpq}$, and that helicity is one-signed, say positive, and maximal, $H_M(k) = E_M(k)/k$. The double constraints of conservation of total E_M and H_M leads to algebraic relations between the energy and helicity interactions between these three wavenumbers. Thus, one obtains:

$$\delta H_{M,k} + \delta H_{M,p} + \delta H_{M,q} = 0 , \quad (2)$$

$$\delta E_{M,k} + \delta E_{M,p} + \delta E_{M,q} = 0 = k\delta H_{M,k} + p\delta H_{M,p} + q\delta H_{M,q} , \quad (3)$$

due to the detailed conservation properties within each triadic interactions. In the specific case chosen here, this gives $\delta H_{M,k} = 2\delta H_{M,q}$, $\delta E_{M,k} = \frac{1}{2}\delta E_{M,q}$. So we conclude that, under these hypotheses, and starting from an excitation at the intermediate scale $\sim 2\pi/p$, there is more magnetic helicity transfer to the large scales $\sim 2\pi/k$, and more magnetic energy transfer to the small scales $\sim 2\pi/q$. This agrees with the fact that, in the forced case, the flux of magnetic helicity is observed to build-up an inverse cascade over time [*Kim and Cho*, 2015]. It should be noted that, when injecting energy of \pm circularly polarized EMHD waves in a system through a forcing mechanism at some scale, one necessarily injects magnetic helicity, which can thus be regarded as a direct consequence of the properties of such waves [*Cho*, 2011]. The ratio of the \pm injection rates, $R_{emhd} = \epsilon_+/\epsilon_- = D_t E_+/D_t E_-$ appears to be the central parameter determining the fate of these flows: the inverse energy cascade is found for $R_{emhd} \approx 1.2$, but instead of a pure self-similar spectrum for the energy, it takes the form of an envelope [*Kim and Cho*, 2015].

A rather novel result in MHD is that in fact the magnetic helicity undergoes constant-flux cascades to both large scales and small scales [*Alexakis et al.*, 2006; *Müller and Malapaka*, 2013]. This was shown using a detailed analysis of the degree of non-locality of nonlinear interactions (see also *Debliquy et al.* [2005]). The flux of magnetic helicity is observed, somewhat remarkably, to remain of a constant sign across the forcing scale, due to the compensating effects of the change of sign of H_M

and that of the flux of H_M across that scale. The nonlocal interactions in MHD are therefore able to smooth-out the process of transfer across the scales. Using Particle In Cell numerical simulations for two-dimensional plasmas including all three components of the fields, it is argued in *Che et al.* [2014], in the context of Solar Wind observations [*Marino et al.*, 2008, 2011], that a dual magnetic energy cascade is observed which is interpreted as being due to wave-wave interactions, kinetic Alfvén waves and whistler waves, which feed both the electron and ion scales due to the anisotropy of the electric and magnetic fields, although no energy fluxes are given to confirm this finding. Anisotropy plays an essential role in this mechanism since the momentum transfer is shown to occur between the perpendicular and parallel components of the magnetic field, each transferring to either larger or smaller scales, in the latter case, with the formation of kinetic-scale micro-current structures, as recently observed.

3.4 The two-dimensional case in MHD

In two dimensions, the purely magnetic invariant, $\langle A^2 \rangle$, is positive definite. In that case, it can be demonstrated phenomenologically, and numerically as well, that the transition between a fluid-dominated to a magnetically dominated regime in the presence of forcing is controlled by the ratio of the kinetic to magnetic energy injection rate, namely $\mu = \epsilon_M/\epsilon_V = D_t E_M/D_t E_V$ [*Seshasanayan and Alexakis*, 2016]. The two-dimensionality of the flow allows for large numerical resolutions, and the critical state is identified explicitly, with the divergence of a susceptibility at the critical “temperature” (here, μ), and power-law scaling close to the critical points, which are slightly different for the change of direct to inverse cascade of magnetic potential and that of kinetic energy.

Specifically, for small magnetic forcing, in this 2D case, there is an inverse cascade of kinetic energy, and the large-scale magnetic energy spectrum corresponds to equipartition of magnetic potential modes (or $E_M(k) \sim k^{+3}$). On the other hand, for strong magnetic forcing, the equipartition is observed in the large-scale kinetic energy, whereas the magnetic potential undergoes an inverse cascade, as first derived in *Fyfe and Montgomery* [1976] and found using two-point closure techniques for turbulence (see review in *Pouquet* [1996]). These differences in spectral behavior have their counterpart in configuration space, with a change in dominant structures according to the value of the critical parameter μ , and in the amount of intermittency as measured through the exact cubic flux laws arising from the conservation laws of energy for the two different underlying systems [*Seshasanayan and Alexakis*, 2016]. It would be of interest to compute as well high-order moments corresponding to the fat tails in the Probability Distribution Functions that are observed to quantify the multi-fractality of these systems, and its disappearance in the inverse cascade. One of the conclusions in *Seshasanayan and Alexakis* [2016] is that there is a range of values of μ for which two regimes cohabit, one mostly fluid, one mostly MHD and with at the same time a flux of energy which is both positive and constant, corresponding to the direct cascade, and negative and constant corresponding to the inverse cascade. Furthermore, two-scale instabilities in both 3D and 2D using Floquet analysis are performed in *Alexakis* [2018]; a stability diagram is built and an overlap region of the two types of instabilities in the laminar case is found which can be linked to the turbulent bi-directional cascade phenomenon as a function of the height of the fluid.

Finally note that the two-dimensional case in the absence of a third component of \mathbf{u} and \mathbf{b} is a bit special in the sense that it does not allow for helical (topological) invariants. However, when including the third component of the fields (vertical velocity and magnetic field), the helicity is non-zero *a priori*, more invariants arise [*Montgomery and Turner*, 1982] and this would deserve further study since this configuration also corresponds to three-dimensional MHD in the presence of a strong uniform magnetic

field. Also note that the spectral index of the inverse cascade can depend on the anisotropy of the forcing for rotating stratified turbulence [Oks *et al.*, 2017].

3.5 The role of anisotropy

There are several issues that merit further attention. One of them concerns the development of anisotropy in such flows. Both an imposed uniform rotation or uniform magnetic field render the flow quasi-bi-dimensional. The resulting anisotropic bi-directional cascade has been studied in detail, with a progressive increase of the inverse (quasi-2D) flux as B_0 increases (see also Favier *et al.* [2011]; Reddy *et al.* [2014], and for the two-dimensional case, Shebalin *et al.* [1983]). It helps in the interpretation of Solar Wind data [Verdini *et al.*, 2015], and has also applications in metallurgy: indeed, it is known that for sufficiently strong B_0 , the fluid behaves like a quasi 2D three-component neutral fluid, the Lorentz force acting as an anisotropic dissipation, together with nonlocal energy transfers between the toroidal and poloidal components of the fields [Favier *et al.*, 2011; Reddy *et al.*, 2014]. It is further found that the perpendicular components of the velocity undergo an upscale cascade whereas its parallel component follows a direct cascade, although this may depend on the strength of B_0 . Such phenomena display a critical behavior [Sujovolsky and Mininni, 2016], the intensity of the magnetic fluctuations increasing as the one-half power of the Alfvén time based on the large-scale flow and on the uniform field. Furthermore, for strong B_0 , the direct cascade is dominated by helicity (in relative terms), as in the rotating case [Mininni and Pouquet, 2009]. It is not clear what happens when both rotation and an imposed uniform magnetic field are present, but the angle between these two imposed fields may alter the dynamics in significant ways. For example, it is shown in Sallai *et al.* [2017] that the Alfvén ratio (that is, the ratio of kinetic to magnetic energy in terms of radial spectra) has a different power-law decay for the parallel and orthogonal cases. It is seen moreover that quasi-equipartition recovers for wavenumbers such that the parameter $V_A k$ be much larger than unity, with V_A the Alfvén velocity associated with the imposed magnetic field, whereas, at large scale, the equipartition is between the kinetic and potential energy for $V_A k/N$ much smaller than unity, with N the Brunt-Väisälä frequency.

4 The bi-directional cascade in rotating stratified flows

Similarly to the MHD case, there is also a bi-directional constant-flux system of energy cascades in rotating stratified turbulence (RST) to both the small scales and the large scales [Pouquet and Marino, 2013; Marino *et al.*, 2015; Pouquet *et al.*, 2017]. One can summarize these results, by analogy to MHD, in the following manner. In the atmosphere and the oceans, energy is injected through solar radiation, tides, bottom topography or winds for example. The large scales of such flows are in a geostrophic balance between pressure gradient, Coriolis force and gravity. This leads to a quasi-2D behavior with the energy flowing to the large scales and thus without a clear way to dissipate the energy, a process which mostly takes place at small scale. What is, then, the mechanism for dissipating the energy in such flows? In the presence of rotation, gravity as well as shear, several instabilities are known to exist; they take their energy from either the kinetic or the potential modes (see Wang *et al.* [2014]; Feraco *et al.* [2018]). These instabilities can be viewed as the premisses of a direct cascade of energy to the small scales, with a constant flux, together with the inverse cascade. For atmospheric and oceanic dynamics, this split process for the energy cascade is essential.

In Figure 2 (top left), we visualize the vorticity structures that develop in rotating stratified turbulence with large-scale eddies due to the influence of the rotation, at the border of which very strong small-scale vortex lanes develop because of instabilities

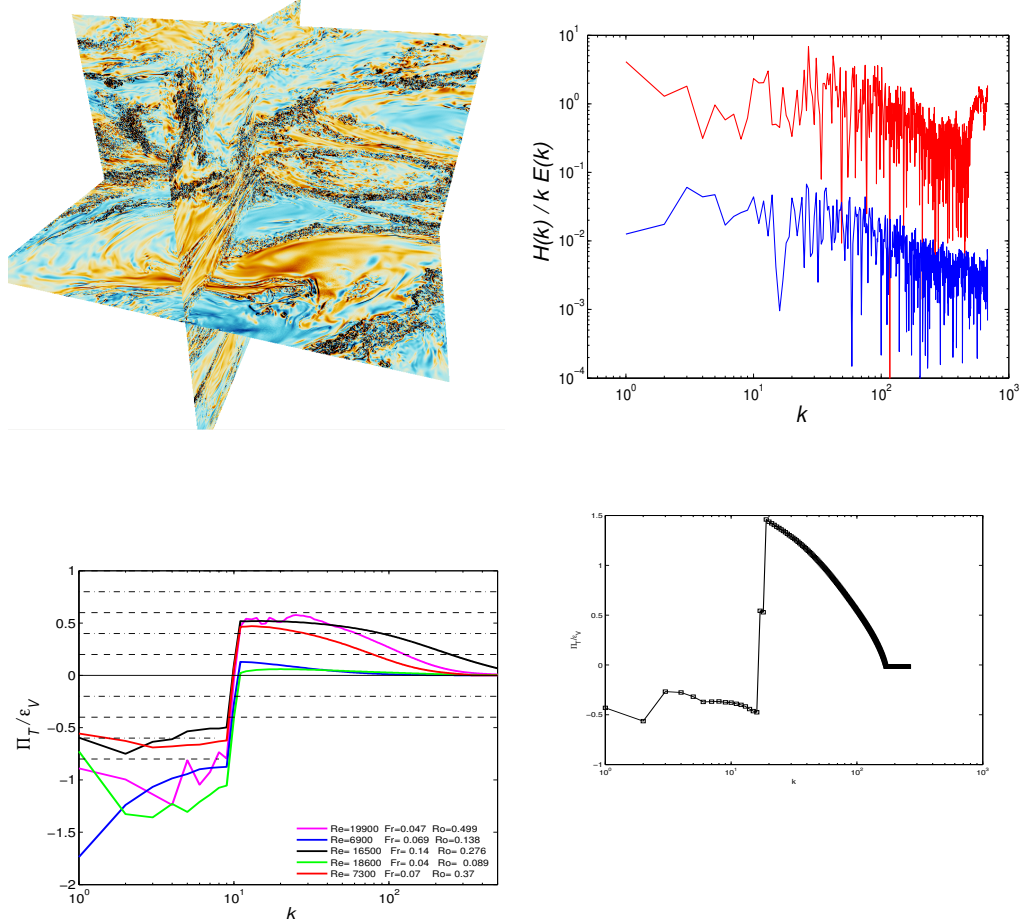


Figure 2. Rotating stratified flows. *Top*: vorticity strength on three planes, color map in Rosenberg *et al.* [2015] (left); relative helicity spectra at two times (right). *Bottom*: Energy flux with dual cascades (parameters in insert) for isotropic (left) and quasi-geostrophic (right) forcing.

such as Kelvin-Helmholtz or those due to shear. The plot is for a flow with $Re \approx 5.5 \times 10^4$, $Fr \approx 0.024$, $Ro \approx 0.1$, for a decay run on a grid of 4096^3 points, integrating the Boussinesq equations (see Rosenberg *et al.* [2015] and references therein for more details). The Reynolds number is defined as the ratio of the dissipation time L_0^2/ν to the turn-over time τ_{NL} previously defined, with ν the viscosity, whereas the Froude and Rossby numbers are defined respectively as the ratio of the period of the wave (gravity or inertial, τ_g, τ_i) to the turn-over time, with $\tau_g = 1/N, \tau_i = 1/f$ where N, f are the Brunt-Väisälä frequency and twice the rotation rate.

For runs with forcing centered on $k_F \approx 10$ and a resolution of 1024^3 grid points, the relative helicity $\sigma_V(k)$ is displayed in Fig. 2 (top right) at two different times, with the data displaced upward by 100 for clarity for the later time; $\sigma_V(k)$ is seen to be independent of wavenumber at large scales, in the inverse cascade, whereas it decays as $\approx 1/k$ at scales smaller than the forcing, as it would for fully developed turbulence. The bi-directional constant total energy flux, normalized by the kinetic energy dissipation ϵ_V , is given for several runs with parameters given in the insert. As analyzed in Pouquet and Marino [2013]; Marino *et al.* [2015]; Pouquet *et al.* [2017], the ratio of the forward to inverse flux varies as $[RoFr]^{-1}$ as long as the Rossby number

is below unity and for buoyancy Reynolds numbers $\mathcal{R}_B = ReFr^2$ above a threshold of order 10. Note that the analysis of the forced case was also shown to be compatible with the energy flux to the small scales being proportional to Fr , when the (total) energy flux to the large scale was inversely proportional to the Rossby number Ro : at fixed Froude number, the stronger the rotation, the more the energy flows to the large scales. Finally, at the bottom right of Fig. 2 is given again the total energy flux, but this time with a forcing in quasi-geostrophic balance. The run is at a lower Reynolds number, and thus the direct flux is competing with dissipation and is not constant at that resolution, but it confirms the generality of the bi-directional cascades in RST.

In terms of oceanic dynamics, the instabilities giving rise to the forward transfer of energy are often identified as sub-meso-scale currents at scales of 1 km which have been recently discovered in the ocean [McWilliams, 2016], and which, in general, are hard to obtain numerically for lack of resolution in global simulations. They may occur in the boundary layers and, if unstable (which they likely are) will provide a path to small dissipative scales, taking the form of eddies, fronts or jets, and filaments. Oceanic observations [Arbic *et al.*, 2013], indicate as well the existence of such a split flux. Such a dual-cascade system can also be viewed as two independent cascades corresponding to the geostrophic and ageostrophic parts of the flow [Bartello, 1995].

Thus, the actual amount of dissipation (as opposed to that expected for a field composed of a superposition of linear waves interacting weakly), affects the overall atmospheric and oceanic energetic exchanges, and it can also modify conditions for acoustic transmission, as well as for deep-water drilling. It is thus an important feature of such flows to be determined. The presence of waves affects directly turbulent flows in lessening the rate at which energy is dissipated; it has been observed in several instances [Campagne *et al.*, 2016; Maffioli *et al.*, 2016; Pouquet *et al.*, 2017], with in the case of rotating stratified flows, a linear dependence of the measured dissipation on the control parameter, the Froude number in an intermediate regime of eddy-wave interactions [Marino *et al.*, 2015; Pouquet *et al.*, 2018], with the Rossby number controlling on the other hand the amount of energy going to the large scales in a simultaneous inverse cascade.

5 Conclusion and Perspectives

The study of turbulence, for fluids and MHD, and of nonlinear systems in general, is progressing substantially. It also leads to the existence of large data sets. An existing approach to reduce the complexity of the problem has been to identify regions of strong turbulent activity in coherent structures, such as with a principal orthogonal decomposition (see Mezić [2013] for a recent review), through intermittency as well as enhanced dissipation such as in current sheets, and concentrate the analysis on such regions. When contemplating the vorticity field [Ishihara *et al.*, 2016], computed on a grid of 4096^3 points (or in excess of 64 billion points), it becomes apparent that the information content of such a picture is enormous, and the dynamics of the fields on such a large grid is computed with spectral accuracy. Analysis of such large data sets is cumbersome; is there another way out? Little has been done in the field of turbulence using modern techniques such as data neural networks, although we already have some pieces of information. Machine Learning (ML) has now been used in fluid turbulence [Duriez *et al.*, 2017], with possible applications to drag reduction for cars, trucks and ships through active turbulent flow control mechanisms. Other applications include the re-“discovery” of the underlying equations from experimental and/or numerical data [Brunton *et al.*, 2017], the development of new and improved sub-grid scale modeling [Ling *et al.*, 2016; Kutz, 2017], or the prediction of long-time behavior of chaotic systems [Pathak *et al.*, 2018].

Various physics-based model enhancements have already been proposed, as for example including helicity-dependent eddy diffusivities [Baerenzung *et al.*, 2008] including in the case of shear flows [Yokoi and Brandenburg, 2016], or when helicity leads to large-scale instabilities [Frisch *et al.*, 1987], or for models including the potential energy for RST [Zilitinkevich *et al.*, 2008]. One application will be to illuminate the possible connection to climate between atmospheric and oceanic dynamics, or in the controlling of uncertainties in RANS (Reynolds-Averaged Navier-Stokes) high-fidelity models through the use of large numerical simulations, either directly exploiting for example a large turbulence data base [Graham *et al.*, 2016; Duraisamy *et al.*, 2018; Wang *et al.*, 2017], or with Large-Eddy Simulations. It may also inform the functional form of the closure schemes, as well as the actual values of the coefficients appearing in such closures.

These approaches are rather unexplored in MHD. Automatized current structure identification was performed in *Servidio et al.* [2010]; *Klimas and Uritsky* [2017] for 2D MHD flows by detecting nulls of the magnetic field with a local hyperbolic topology as the plausible locus of reconnection events. Similarly, one can observe geo-dynamo field reversals using a decomposition of the data through a chaotic forcing with strong intermittent bursts [Brunton *et al.*, 2017]. Finally, Lagrangian models (also called α -models) allow for computations at high Reynolds numbers by introducing a filter length-scale that may lead to extended regions of very weak nonlinear transfer [Mininni *et al.*, 2005], and ML procedures could alleviate that problem. What about incorporating cross-helicity and/or magnetic helicity in transport coefficients for MHD, following similar venues?

In what way will existing machine learning algorithms change in the presence of inverse cascades? How will such modeling be affected by the existence of bi-directional cascades? Much remains to be learned but it seems rather certain that Big Data and Data Science will play a role in MHD turbulence, as it may be able to play a role in other fields. These issues could be investigated soon with the existence, as mentioned earlier, of new observational small-scale data with the Multiscale Magnetospheric mission [Wilder *et al.*, 2016; Chasapis *et al.*, 2017; Ergun *et al.*, 2018; Gershman *et al.*, 2018]), with experimental data (*e.g.*, coming from the Coriolis table [Aubourg *et al.*, 2017]), and with numerical data stemming from high-performance computing studies of FDT [Ishihara *et al.*, 2016], of rotating and/or stratified turbulence [de Bruyn Kops, 2015; Rosenberg *et al.*, 2015], as well as of turbulent interfaces in RST [Watanabe *et al.*, 2016], and of MHD turbulence [Beresniak, 2014].

Acknowledgments

RM acknowledges financial support from PALSE (Programme Avenir Lyon Saint-Etienne) of the University of Lyon, in the framework of the program Investissements d'Avenir (ANR-11-IDEX-0007). Support for AP from LASP, and in particular from Bob Ergun, is gratefully acknowledged. Computations were performed at LASP, on the Janus supercomputer at the University of Colorado (Boulder) for Fig. 1, and at DOE for Fig. 2; they are both thanked. NCAR is supported by NSF, and JES is supported by STFC(UK) grant ST/N000692/1. Data is available from the authors.

References

Abramenko, V., and V. Yurchyshyn (2010), Intermittency and multifractality spectra of the magnetic field in solar active regions, *Astrophys. J.*, 722, 122–130.

Alexakis, A. (2017), Helically decomposed turbulence, *J. Fluid Mech.*, 812, 752–770.

Alexakis, A. (2018), 3D instabilities and negative eddy viscosity in thin-layer flows, *Preprint, see ArXiv:1806:00409v1*.

Alexakis, A., P. Mininni, and A. Pouquet (2006), On the inverse cascade of magnetic helicity, *Astrophys. J.*, **640**, 335–343.

Alexandrova, O., A. Mangeney, M. Maksimovic, N. Cornilleau-Wehrlin, J.-M. Bosqued, and M. André (2006), Alfvén vortex filaments observed in magnetosheath downstream of a quasi-perpendicular bow shock, *J. Geophys. Res.*, **111**(A12208).

Arbic, B., K. Polzin, R. Scott, J. Richman, and J. Shriver (2013), On eddy viscosity, energy cascades, and the horizontal resolution of gridded satellite altimeter products, *J. Phys. Oceano.*, **43**, 283–300.

Aubourg, Q., A. Campagne, C. Peureux, F. Arduin, J. Sommeria, S. Viboud, and N. Mordant (2017), Three-wave and four-wave interactions in gravity wave turbulence, *Phys. Rev. Fluids*, **2**, 114,802.

Baerenzung, J., H. Politano, Y. Ponty, and A. Pouquet (2008), Spectral modeling of turbulent flows and the role of helicity, *Phys. Rev. E*, **77**, 046,303.

Bartello, P. (1995), Geostrophic adjustment and inverse cascade in rotating stratified turbulence, *J. Atmos. Sci.*, **52**, 4410–4428.

Beresniak, A. (2014), Spectra of strong magnetohydrodynamic turbulence from high resolution simulations, *Astrophys. J. Lett.*, **784**(L20).

Biferale, L., and E. Titi (2013), On the global regularity of a helical-decimated version of the 3D Navier-Stokes equations, *J. Stat. Phys.*, **151**, 1089–1098.

Biferale, L., S. Musacchio, and F. Toschi (2012), Inverse energy cascade in three-dimensional isotropic turbulence, *Phys. Rev. Lett.*, **108**, 164,501.

Blackman, E. (2015), Magnetic helicity and large scale magnetic fields: A primer, *Space Sci. Rev.*, **8**.

Bratanov, V., F. Jenko, D. R. Hatch, and M. Wilczek (2013), Non-universal power-law spectra in turbulent systems, *Phys. Rev. Lett.*, **111**, 075,001.

Briard, A., and T. Gomez (2018), The decay of isotropic magnetohydrodynamic turbulence and the effects of cross-helicity, *J. Plasma Phys.*, **84**, 905840,110.

Brunton, S. L., B. W. Brunton, J. L. Proctor, E. Kaiser, and J. N. Kutz (2017), Chaos as an intermittently forced linear system, *Nature Comm.*, **8**, 1–9.

Campagne, A., N. Machicoane, B. Gallet, P. P. Cortet, and F. Moisy (2016), Turbulent drag in a rotating frame, *J. Fluid Mech.*, **794**, R5.

Cassak, P. A., A. Emslie, A. Halford, D. Baker, H. Spence, S. Avery, and L. Fisk (2017), Space physics and policy for contemporary society, *J. Geophys. Res.*, **122**, 1–6.

Chasapis, C., W. H. Matthaeus, T. N. Parashar, S. A. Fuselier, B. A. Maruca, T. D. Phan, J. L. Burch, T. E. Moore, C. J. Pollock, D. J. Gershman, R. B. Torbert, C. T. Russell, and R. J. Strangeway (2017), High-resolution statistics of Solar Wind turbulence at kinetic scales using the Magnetospheric Multiscale Mission, *Astrophys. J. Lett.*, **844**, L9.

Che, H., M. Goldstein, and A. Viñas (2014), Bidirectional energy cascades and the origin of kinetic Alfvénic and whistler turbulence in the solar wind, *Phys. Rev. Lett.*, **112**, 061,101.

Chen, Q., S. Chen, and G. Eyink (2003), The joint cascade of energy and helicity in three-dimensional turbulence, *Phys. Fluids*, **15**, 361–374.

Childresss, S., and A. D. Gilbert (1995), *Stretch, Twist, Fold: The Fast Dynamo, LNP*, vol. 37, Springer.

Cho, J. (2011), Magnetic helicity conservation and inverse energy cascade in electron magnetohydrodynamic wave packets, *Phys Rev. Lett.*, **106**, 191,104.

Choi, Y., Y. Lvov, S. Nazarenko, and B. Pokorni (2005), Anomalous probability of large amplitudes in wave turbulence, *Phys. Lett. A*, **339**, 361–369.

Clark di Leoni, P., P. Cobelli, and P. D. Mininni (2017), The spatio-temporal spectrum of turbulent flows, *Eur. Phys. J. E*, p. Preprint.

Collaboration SHREK: B. Saint-Michel, E. Herbert, J. Salort, C. Baudet, M. B. Mardion, P. Bonnay, M. Bourgoin, B. Castaing, L. Chevillard, F. Daviaud, P. Diribarne,

B. Dubrulle, and Y. Gagne (2014), Probing quantum and classical turbulence analogy through global bifurcations in a von Kàrmà̄n liquid Helium experiment, *Phys. Fluids*, *26*(125109).

Constantinescu, G., S. Miyawaki, B. Rhoads, A. Sukhodolov, and G. Kirkil (2011), Structure of turbulent flow at a river confluence with momentum and velocity ratios close to 1: Insight provided by an eddy-resolving numerical simulation, *Water Resources Res.*, *47*(W05507), 1–16.

Dallas, V., and A. Alexakis (2015), Self-organisation and non-linear dynamics in driven magnetohydrodynamic turbulent flows, *Phys. Fluids*, *27*, 045,105.

de Bruyn Kops, S. (2015), Classical scaling and intermittency in strongly stratified Boussinesq turbulence, *J. Fluid Mech.*, *775*, 436–463.

Debliquy, O., M. Verma, and D. Carati (2005), Energy fluxes and shell-to-shell transfers in three-dimensional decaying magnetohydrodynamic turbulence, *Phys. Plasmas*, *12*, 042,309.

Duraisamy, K., G. Iaccarino, and H. Xiao (2018), Turbulence modeling in the age of data, *Ann. Rev.*, *preprint*, *ArXiv:1804:00183v1*, pp. 1–23.

Duriez, T., S. L. Brunton, and B. R. Noack (2017), *Machine Learning Control – Taming Nonlinear Dynamics and Turbulence, Fluid Mechanics and its Applications*, vol. 116, Springer.

Ergun, R. E., K. A. Goodrich, F. D. Wilder, N. Ahmadi, J. C. Holmes, S. Eriksson, J. E. Stawarz, R. Nakamura, K. J. Genestreti, M. Hesse, J. L. Burch, R. B. Torbert, T. D. Phan, S. J. Schwartz, J. P. Eastwood, R. J. Strangeway, O. L. Contel, C. T. Russell, M. Argall, P. A. Lindqvist, L. J. Chen, P. A. Cassak, B. L. Giles, J. C. Dorelli, D. Gershman, T. W. Leonard, B. Lavraud, A. Retino, W. Matthaeus, and A. Vaivads (2018), Magnetic reconnection, turbulence, and particle acceleration: Observations in the Earth's magnetotail, *Geophys. Res. Lett.*, *45*, 3338–3347.

Favier, B., F. Godeferd, C. Cambon, A. Delache, and W. Bos (2011), Quasi-static magnetohydrodynamic turbulence at high Reynolds number, *J. Fluid Mech.*, *681*, 434–461.

Feraco, F., R. Marino, A. Pumir, L. Primavera, P. Mininni, A. Pouquet, and D. Rosenberg (2018), Vertical drafts and mixing in stratified turbulence: sharp transition with Froude number, *Preprint, see ArXiv:1806.00342v1*.

Fjørtoft, R. (1953), On the changes in the spectral distribution of kinetic energy for two-dimensional non-divergent flows, *Tellus*, *5*, 225–230.

Frisch, U., A. Pouquet, J. Léorat, and A. Mazure (1975), Possibility of an inverse cascade of magnetic helicity in magnetohydrodynamic turbulence, *J. Fluid Mech.*, *68*, 769–778.

Frisch, U., Z. She, and P. Sulem (1987), Large-scale flow driven by the anisotropic kinetic alpha effect, *Physica D*, *28*, 382–392.

Fyfe, D., and D. Montgomery (1976), High beta turbulence in two-dimensional magnetohydrodynamic, *J. Plasma Phys.*, *16*, 181–191.

Galtier, S. (2012), Kolmogorov vectorial law for Solar Wind turbulence, *Astrophys. J.*, *746*, 184.

Galtier, S., and A. Bhattacharjee (2003), Anisotropic weak whistler wave turbulence in electron magnetohydrodynamics, *Phys. Plasmas*, *10*, 3065–3076.

Gershman, D. J., A. F.-Viñas, J. C. Dorelli, M. L. Goldstein, J. Shuster, L. A. Avanov, S. A. Boardsen, J. E. Stawarz, S. J. Schwartz, C. Schiff, B. Lavraud, Y. Saito, W. R. Paterson, B. L. Giles, C. J. Pollock, R. J. Strangeway, C. T. Russell, R. B. Torbert, T. E. Moore, and J. L. Burch (2018), Energy partitioning constraints at kinetic scales in low- β turbulence, *Phys. Plasmas*, *25*, 022,303.

Gibson, S., and Y. Fan (2008), Partially ejected flux ropes: Implications for interplanetary coronal mass ejections, *J. Geophys. Res.*, *113*, A09,103.

Graham, J., K. Kanov, X.I.A. Yang, M. Lee, N. Malaya, C. Lalescu, R. Burns, G. Eyink, A. Szalay, R. Moser, and C. Meneveau (2016), A Web services accessible database

of turbulent channel flow and its use for testing a new integral wall model for LES, *J. Turbulence*, *17*, 181–215.

Gustavsson, K., and L. Biferale (2016), Preferential sampling of helicity by isotropic helicoids, *Phys. Rev. F*, *1*, 054,201.

Henri, P., F. Califano, C. Briand, and A. Mangeney (2011), Low-energy Langmuir cavitons: Asymptotic limit of weak turbulence, *Eur. J. Phys. Lett.*, *96*, 55,004.

Hide, R. (2002), Helicity, superhelicity and weighted relative potential vorticity: Useful diagnostic pseudoscalars?, *Q. J. Roy. Met. Soc.*, *128*, 1759–1762.

Higashimori, K., N. Yokoi, and M. Hoshino (2013), Explosive turbulent magnetic reconnection, *Phys. Rev. Lett.*, *110*(255001).

Howes, G., and E. Quataert (2010), On the interpretation of magnetic helicity signatures in the dissipation range of Solar Wind turbulence, *Astrophys. J. Lett.*, *709*, L49–L52.

Ishihara, T., K. Morishita, M. Yokokawa, A. Uno, and Y. Kaneda (2016), Energy spectrum in high-resolution direct numerical simulations of turbulence, *Phys. Rev. F*, *1*(082403(R)).

Iyer, K. P., K. R. Sreenivasan, and P. K. Yeung (2017), Reynolds number scaling of velocity increments in isotropic turbulence, *Phys. Rev. E*, *95*, 021,101(R).

Karimabadi, H., V. Roytershteyn, M. Wan, W. H. Matthaeus, W. Daughton, P. Wu, M. Shay, B. Loring, J. Borovsky, E. Leonardis, S. C. Chapman, and T. K. M. Nakamura (2013), Coherent structures, intermittent turbulence, and dissipation in high-temperature plasmas, *Phys. Plasmas*, *20*, 012,303.

Kim, H., and J. Cho (2015), Inverse cascade in imbalanced electron magnetohydrodynamic turbulence, *Astrophys. J. Suppl.*, *801*, 75.

Klimas, A. J., and V. M. Uritsky (2017), Criticality and turbulence in a resistive magnetohydrodynamic current sheet, *Phys. Rev. E*, *95*, 023,209.

Kraichnan, R. (1967), Inertial ranges in two-dimensional turbulence, *Phys. Fluids*, *10*, 1417–1423.

Kraichnan, R. (1973), Helical turbulence and absolute equilibrium, *J. Fluid Mech.*, *59*, 745–752.

Kutz, J. (2017), Deep learning in fluid dynamics, *J. Fluid Mech.*, *814*, 1–4.

Lee, E., M. Brachet, A. Pouquet, P. Mininni, and D. Rosenberg (2010), On the lack of universality in decaying magnetohydrodynamic turbulence, *Phys. Rev. E*, *81*, 016,318.

Levina, G., and M. Montgomery (2014), Tropical cyclogenesis: a numerical diagnosis based on helical flow organization, *J. Phys: Conf. Ser.*, *544*, 012,013.

Ling, J., A. Kurzawski, and J. Templeton (2016), Reynolds averaged turbulence modelling using deep neural networks with embedded invariance, *J. Fluid Mech.*, *807*, 155–166.

Loureiro, N. F., A. A. Schekochihin, and D. A. Uzdensky (2013), Plasmoid and Kelvin-Helmholtz instabilities in Sweet-Parker current sheets, *Phys. Rev. E*, *87*, 013,102.

Maffioli, A., G. Brethouwer, and E. Lindborg (2016), Mixing efficiency in stratified turbulence, *J. Fluid Mech.*, *794*, R3.

Malapaka, S., and W. Müller (2013), Modeling statistical properties of solar active regions through direct numerical simulations of 3D-MHD turbulence, *Astrophys. J.*, *774*, 84.

Marino, R., L. Sorriso-Valvo, V. Carbone, A. Noullez, R. Bruno, and B. Bavassano (2008), Heating the solar wind by a magnetohydrodynamic turbulent energy cascade, *Astrophys. J.*, *677*, L71.

Marino, R., L. Sorriso-Valvo, V. Carbone, P. Veltri, A. Noullez, and R. Bruno (2011), The magnetohydrodynamic turbulent cascade in the ecliptic solar wind: Study of Ulysses data, *Planetary and Space Sc.*, *59*, 592–597.

Marino, R., P. Mininni, D. Rosenberg, and A. Pouquet (2013), Emergence of helicity in rotating stratified turbulence, *Phys. Rev. E*, *87*, 033,016.

Marino, R., A. Pouquet, and D. Rosenberg (2015), Resolving the paradox of oceanic large-scale balance and small-scale mixing, *Phys. Rev. Lett.*, **114**, 114,504.

Matthaeus, W., and M. Goldstein (1982), Measurement of the rugged invariants of magnetohydrodynamic turbulence in the Solar Wind, *J. Geophys. Res.*, **87**, 6011–6028.

McWilliams, J. (2016), Submesoscale currents in the ocean, *Proc. Roy. Soc. A*, **472**, 2016.0117.

Meyrand, R., K. H. Kiyani, and S. Galtier (2015), Weak magnetohydrodynamic turbulence and intermittency, *J. Fluid Mech.*, **770**, R1, 1–11.

Mezić, I. (2013), Analysis of fluid flows via spectral properties of the Koopman operator, *Ann. Rev. Fluid Mech.*, **45**, 357–378.

Mininni, P., and A. Pouquet (2009), Helicity cascades in rotating turbulence, *Phys Rev E*, **79**, 026,304.

Mininni, P., A. Pouquet, and D. Montgomery (2006), Small-scale structures in three-dimensional magnetohydrodynamic turbulence, *Phys. Rev. Lett.*, **97**, 244,503.

Mininni, P. D., and A. Pouquet (2007), Energy spectra stemming from interactions of Alfvén waves and turbulent eddies, *Phys. Rev. Lett.*, **99**, 254,502.

Mininni, P. D., D. Montgomery, and A. Pouquet (2005), Numerical solutions of the three-dimensional MHD alpha model, *Phys. Rev. E*, **71**, 046,304.

Moffatt, H., and A. Tsinober (1992), Helicity in laminar and turbulent flow, *Ann. Rev. Fl. Mech.*, **24**, 281–312.

Molinari, J., and D. Vollaro (2010), Distribution of helicity, CAPE, and shear in tropical cyclones, *J. Atmos. Sci.*, **67**, 274–284.

Montgomery, D., and L. Turner (1982), Two-and-a-half dimensional magnetohydrodynamic turbulence, *Phys Fluids*, **25**, 345–349.

Morrison, I., S. Businger, F. Marks, P. Dodge, and J. A. Businger (2005), An observational case for the prevalence of roll vortices in the hurricane boundary layer, *J. Atmos. Sci.*, **62**, 2662–2673.

Müller, W., and S. Malapaka (2013), Role of helicities for the dynamics of turbulent magnetic fields, *Geophys. Astrophys. Fluid Dyn.*, **107**, 93–100.

Newell, A., and V. Zakharov (2008), The role of the generalized Phillips spectrum in wave turbulence, *Phys. Lett. A*, **372**, 4230–4233.

Nore, C., M. B. H. Politano, and A. Pouquet (1997), Dynamo action in a Taylor-Green vortex near threshold, *Phys. Plasmas Lett.*, **4**, 1–3.

Oks, D., P. Mininni, R. Marino, and A. Pouquet (2017), Inverse cascades and resonant triads in rotating and stratified turbulence, *Phys. Fluids*, **29**, 111,109.

Osman, K. T., W. H. Matthaeus, J. T. Gosling, A. Greco, S. Servidio, B. Hnat, S. C. Chapman, and T. D. Phan (2014), Magnetic reconnection and intermittent turbulence in the solar wind, *Phys. Rev. Lett.*, **112**, 215,002.

Pathak, J., B. Hunt, M. Girvan, Z. Lu, and E. Ott (2018), Model-free prediction of large spatiotemporally chaotic systems from data: A reservoir computing approach, *Phys. Rev. Lett.*, **120**, 024,102.

Perez, J. C., J. Mason, S. Boldyrev, and F. Cattaneo (2014), Scaling properties of small-scale fluctuations in magnetohydrodynamic turbulence, *Astrophys. J. Lett.*, **793**(L13).

Phan, T. D., J. P. Eastwood, M. A. Shay, J. F. Drake, B. U. Ö. Sonnerup, M. Fujimoto, P. A. Cassak, M. Øieroset, J. L. Burch, R. B. Torbert, A. C. Rager, J. C. Dorelli, D. J. Gershman, C. Pollock, P. S. Pyakurel, C. C. Haggerty, Y. Khotyaintsev, B. Lavraud, Y. Saito, M. Oka, R. E. Ergun, A. Retino, O. Le Contel, M. R. Argall, B. L. Giles, T. E. Moore, F. D. Wilder, R. J. Strangeway, C. T. Russell, P. A. Lindqvist, and W. Magnes (2018), Electron magnetic reconnection without ion coupling in Earth’s turbulent magnetosheath, *Nature*, **557**, 202–206.

Porter, D., A. Pouquet, and P. Woodward (2002), Intermittency in compressible flows, *Phys. Rev. E*, **66**, 026,301.

Pouquet, A. (1993), Magnetohydrodynamic turbulence, in *Les Houches Summer School on Astrophysical Fluid Dynamics, July 1987. Session XLVII*, edited by J. P. Zahn and J. Zinn-Justin, pp. 139–227, Elsevier.

Pouquet, A. (1996), Turbulence, statistics and structures: an introduction, in *Vth European School in Astrophysics, San Miniato; Lecture Notes in Physics “Plasma Astrophysics” vol. 468*, edited by C. Chiuderi and G. Einaudi, pp. 163–212, Springer-Verlag.

Pouquet, A., and R. Marino (2013), Geophysical turbulence and the duality of the energy flow across scales, *Phys. Rev. Lett.*, *111*, 234,501.

Pouquet, A., U. Frisch, and J. Léorat (1976), Strong MHD helical turbulence and the nonlinear dynamo effect, *J. Fluid Mech.*, *77*, 321–354.

Pouquet, A., M. Meneguzzi, and P. L. Sulem (1988), Influence of velocity-magnetic field correlations on decaying magnetohydrodynamic turbulence with neutral X-points, *Phys. Fluids*, *31*, 2635–2643.

Pouquet, A., R. Marino, P. D. Mininni, and D. Rosenberg (2017), Dual constant-flux energy cascades to both large scales and small scales, *Phys. Fluids*, *29*(111108).

Pouquet, A., D. Rosenberg, R. Marino, and C. Herbert (2018), Scaling laws for mixing and dissipation in unforced rotating stratified turbulence, *J. Fluid Mech.*, *844*, 519–545.

Reddy, K. S., R. Kumar, and M. K. Verma (2014), Anisotropic energy transfers in quasi-static magnetohydrodynamic turbulence, *Phys. Plasmas*, *21*, 102,310.

Reinken, H., S. H. L. Klapp, M. Bär, and S. Heidenreich (2018), Derivation of a hydrodynamic theory for mesoscale dynamics in microswimmer suspensions, *Phys. Rev. E*, *97*, 022,613.

Rorai, C., P. Mininni, and A. Pouquet (2014), Turbulence comes in bursts in stably stratified flows, *Phys. Rev. E*, *89*, 043,002.

Rosenberg, D., A. Pouquet, R. Marino, and P. Mininni (2015), Evidence for Bolgiano-Obukhov scaling in rotating stratified turbulence using high-resolution direct numerical simulations, *Phys. Fluids*, *27*, 055,105.

Salhi, A., F. S. Baklouti, F. Godeferd, T. Lehner, and C. Cambon (2017), Energy partition, scale by scale, in magnetic Archimedes Coriolis weak wave turbulence, *Phys. Rev. E*, *95*, 023,112.

Saur, J., H. Politano, A. Pouquet, and W. Matthaeus (2002), Evidence of weak MHD turbulence in the magnetosphere of Jupiter, *Astron. Astrophys.*, *386*, 699–708.

Servidio, S., W. H. Matthaeus, M. A. Shay, P. Dmitruk, P. A. Cassak, and M. Wan (2010), Statistics of magnetic reconnection in two-dimensional magnetohydrodynamic turbulence, *Phys. Plasmas*, *17*, 032,315.

Seshasanay, K., and A. Alexakis (2016), Critical behavior in the inverse to forward energy transition in two-dimensional magnetohydrodynamic flow, *Phys. Rev. E*, *93*, 013,104.

Shebalin, J., W. Matthaeus, and D. Montgomery (1983), Anisotropy in mhd turbulence due to a mean magnetic field, *J. Plasma Phys.*, *29*, 525–547.

Ślomka, J., and J. Dunkel (2017), Spontaneous mirror-symmetry breaking induces inverse energy cascade in 3D active fluids, *Proc. Nat. Acad. Sci.*, *114*, 2119–2124.

Stawarz, J., and A. Pouquet (2015), Small-scale behavior of Hall magnetohydrodynamic turbulence, *Phys. Rev. E*, *92*, 063,102.

Stawarz, J., C. Smith, B. Vasquez, M. Forman, and B. MacBride (2009), The turbulent cascade and proton heating in the Solar Wind at a AU, *Astrophys. J.*, *697*, 1119–1127.

Stawarz, J. E., R. E. Ergun, and K. A. Goodrich (2015), Generation of high frequency electric field activity by turbulence in the Earth’s magnetotail, *J. Geophys. Res.*, *120*, 1845–1866.

Steenbeck, M., F. Krause, and K.-H. Rädler (1966), Berechnung der mittleren Lorentz-feldstärke $\mathbf{v} \times \mathbf{b}$ für ein elektrisch leitendes medium in turbulenter, durch Coriolis-

Kräfte beeinflusster bewegung, *Z. Naturforsch. A*, *21*, 369–376.

Stenzel, R., J. Urrutia, and C. L. Rousculp (1995), Helicities of electron magnetohydrodynamic currents and fields in plasmas, *Phys. Rev. Lett.*, *74*, 702–705.

Sujovolsky, N., and P. Mininni (2016), Tridimensional to bidimensional transition in magnetohydrodynamic turbulence with a guide field and kinetic helicity injection, *Phys. Rev. F*, *1*, 054,407.

Taylor, J. B. (1986), Relaxation and magnetic reconnection in plasmas, *Rev. Mod. Phys.*, *58*, 741–763.

Ting, A., W. Matthaeus, and D. Montgomery (1986), Turbulence relaxation processes in magnetohydrodynamics, *Phys. Fluids*, *26*, 3261–3274.

Tsurutani, B. T., R. Hajra, T. Tanimori, A. Takada, R. Bhanu, A. J. Mannucci, G. S. Lakhina, J. U. Kozyra, K. Shiokawa, L. C. Lee, E. Echer, R. V. Reddy, and W. D. Gonzalez (2016), Heliospheric plasma sheet (HPS) impingement onto the magnetosphere as a cause of relativistic electron dropouts (REDs) via coherent EMIC wave scattering with possible consequences for climate change mechanisms, *J. Geophys. Res.*, *121*, 1–27.

Valet, J.-P., and A. Fournier (2016), Deciphering records of geomagnetic reversals, *Rev. Geophys.*, *54*, 410–446.

Veltri, P., V. Carbone, F. Lepreti, and G. Nigro (2009), *Self-Organization in Magnetohydrodynamic Turbulence*, R.A. Meyers Ed., Springer.

Verdini, A., R. Grappin, P. Hellinger, S. Landi, and W. C. Müller (2015), Anisotropy of third-order sturcture functions in MHD turbulence, *Astrophys. J.*, *804*, 119.

Waleffe, F. (1992), The nature of triad interactions in homogeneous turbulence, *Phys. Fluids*, *A4*, 350–363.

Wang, J.-X., J.-L. Wu, and H. Xiao (2017), Physics-informed machine learning approach for reconstructing Reynolds-stress modeling discrepancies based on DNS data, *Phys. Rev. F*, *2*, 034,603.

Wang, P., J. C. McWilliams, and C. Ménesguen (2014), Ageostrophic instability in rotating, stratified interior vertical shear flows, *J. Fluid Mech.*, *755*, 397–428.

Watanabe, T., J. R. Riley, S. M. de Bruyn-Kops, P. J. Diamessis, and Q. Zhou (2016), Turbulent/non-turbulent interfaces in wakes in stably stratified fluids, *J. Fluid Mech.*, *797*, R1.

Wensink, H. H., J. Dunkel, S. Heidenreich, K. Drescher, R. E. Goldstein, H. Löwen, and J. M. Yeomans (2012), Meso-scale turbulence in living fluids, *Proc. Nat. Acad. Sci.*, *109*, 14,308–14,313.

Wilder, F. D., R. E. Ergun, K. A. Goodrich, M. V. Goldman, D. L. Newman, D. M. Malaspina, A. N. Jaynes, S. J. Schwartz, K. J. Trattner, J. L. Burch, M. R. Argall, R. B. Torbert, P.-A. Lindqvist, G. Marklund, and O. L. Contel (2016), Observations of whistler mode waves with nonlinear parallel electric fields near the dayside magnetic reconnection separatrix by the Magnetospheric Multiscale mission, *Geophys. Res. Lett.*, *43*, 5909–5917.

Woltjer, L. (1960), On the theory of hydromagnetic equilibrium, *Rev. Mod. Phys.*, *32*, 914–915.

Yokoi, N., and A. Brandenburg (2016), Large-scale flow generation by inhomogeneous helicity, *Phys. Rev. E*, *93*, 033,125.

Yokoi, N., and A. Yoshizawa (1993), Statistical analysis of the effects of helicity in inhomogeneous turbulence, *Phys. Fluids*, *A5*, 464–477.

Zhou, Y., W. Matthaeus, and P. Dmitruk (2004), MHD turbulence and time scales in astrophysical and space plasmas, *Rev. Mod. Phys.*, *76*, 1015–1035.

Zilitinkevich, S. S., T. Elperin, N. Kleerorin, I. Rogachevskii, I. Esau, T. Mauritzen, and M. W. Miles (2008), Turbulence energetics in stably stratified geophysical flows: Strong and weak mixing regimes, *Quart. J. Met. Roy. Soc.*, *134*, 793–799.